



ELSEVIER

Journal of Non-Crystalline Solids 203 (1996) 19–26

JOURNAL OF  
NON-CRYSTALLINE SOLIDS

## Analysis of OH absorption bands in synthetic silica

O. Humbach<sup>a</sup>, H. Fabian<sup>a,\*</sup>, U. Grzesik<sup>a</sup>, U. Haken<sup>a</sup>, W. Heitmann<sup>b</sup>

<sup>a</sup> Heraeus Quarzglas GmbH, Division PLW, P.O. Box 1554, D-63405 Hanau, Germany

<sup>b</sup> Deutsche Telekom AG, Forschungs- und Technologiezentrum, P.O. Box 100003, D-64276 Darmstadt, Germany

### Abstract

The presence of bound hydroxyl (SiOH) in silica is well known to produce an optical fundamental absorption band at about 2.7  $\mu\text{m}$ . For optical fiber applications the influence of the corresponding overtones and combination modes on the absorption spectrum are of significant importance. A literature review is presented which reveals uncertainties regarding the correct absorption band intensities as well as their spectral positions. We present precise data on spectral position and relative intensities of OH absorption bands in state of the art synthetic silica. Our investigations cover the influence of different manufacturing techniques, OH content, and a comparison of bulk and fiber data. With the knowledge of the conversion factors between the intensities of different OH absorption bands it is possible to predict the entire OH related transmission performance of an optical component by measurement of a single absorption band, e.g., the fundamental mode at 2.7  $\mu\text{m}$  or the 1.38  $\mu\text{m}$  band in the low loss range of optical fibers.

### 1. Introduction

The development of optical fibers for telecommunication and high power laser applications has changed the specifications for transmission properties of silica optical components. Only synthetic silica is capable of meeting the requirements of most state of the art technologies. Even in the production of synthetic silica there is still some moisture or hydrogen present in the manufacturing process resulting in hydroxyl groups chemically bonded to the silica network (SiOH). This hydroxyl affects the optical properties of silica due to the fundamental OH absorption band at 2.72  $\mu\text{m}$ , the corresponding overtones and the combination modes with the SiO<sub>4</sub> tetrahedron vibration.

Optical fibers for telecommunication require the highest purity and extremely low OH content. The development of very large preforms manufactured by the MCVD technology [1] was only possible due to the availability of synthetic silica tubing. With increasing preform size the core diameter is enlarged whereas the MCVD cladding thickness is reduced because of the limited amount of silica produced by MCVD. The penetration depth of the lightwave into the starting tube material increases. The performance of such optical fibers is strongly affected by the tube quality, e.g., purity and OH content.

For manufacturing synthetic silica tubing and preforms, it is important to know the influence of OH absorption bands on transmission properties of optical fibers precisely. With such a data base it is possible to extrapolate from bulk to fiber samples and from one spectral wavelength region to another. It may enable the preform manufacturer to estimate

\* Corresponding author. Tel.: +49-6181 367 252; fax: +49-6181 39 420.

the OH absorption peak at 1.38  $\mu\text{m}$  in a fiber by measurements on the preform at 2.72  $\mu\text{m}$ .

The main purpose of this work was to measure the relative intensities of the OH bands in synthetic silica with state of the art equipment. We will not investigate the molar extinction coefficient to obtain absolute values for the OH content. The basic idea is to combine different set-ups, wet and dry silica, bulk and fiber samples, and silica manufactured by different production techniques to obtain precise and complete data on shape, position and relative intensity of OH absorption bands in silica.

## 2. Literature review

OH absorption has been discussed in the literature for decades. Most work has focussed on OH band intensity, spectral position or shape. Determination of absolute hydroxyl content requires knowledge of the extinction coefficient. Most authors use the value of 77.5  $\text{l mol}^{-1} \text{cm}^{-1}$  measured by Stephenson and Jack [2,3], which is however still under discussion [4,5]. Extinction coefficients of 90  $\text{l mol}^{-1} \text{cm}^{-1}$  [6], 70  $\text{l mol}^{-1} \text{cm}^{-1}$  [7] and 58  $\text{l mol}^{-1} \text{cm}^{-1}$  [8] and values ranging from 34 to 86  $\text{l mol}^{-1} \text{cm}^{-1}$  [9] were published. Assuming an OH content of 1 ppm weight

an extinction coefficient of 77.5  $\text{l mol}^{-1} \text{cm}^{-1}$  would lead to additional attenuation of 10000 dB/km at the fundamental OH band at 2.72  $\mu\text{m}$ .

Due to the typical length of optical fibers only the optical loss at the overtone wavelengths has been determined with standard measurements, e.g., 1.38  $\mu\text{m}$  or 0.94  $\mu\text{m}$ . A literature review (see Table 1) reveals variations of the measured optical loss per ppm OH, for example at 0.94  $\mu\text{m}$ . Attenuation values of 0.83 dB/km ppm [12], 1.25 dB/km ppm [10,11,13] and 2 dB/km ppm [14] are reported for fiber and bulk materials (see Table 1).

The spectral position of the OH bands is reported to be influenced by the chemical composition of the silica sample, e.g., concentration of germanium, molecular hydrogen or water [15–17]. The fundamental and combination modes of the  $\text{SiO}_4$  tetrahedron vibration were found to be shifted as a function of fictive temperature [18–21]. The sum frequencies of those tetrahedron modes and OH vibrations are called OH combination modes. One may conclude that these OH combination modes should also be affected by fictive temperature but we did not find any data in the literature.

Investigations of the shape of the first OH overtone band at 1.38  $\mu\text{m}$  show that it can be decomposed into four Gaussians or into combinations of

Table 1  
Comparison between literature data on OH band positions and extinction coefficients in silica <sup>a</sup>

OH band ident.	Keck et al. [10,11] <sup>b</sup>		Kaiser et al. [12] <sup>c</sup>		Elliott et al. [13]		Clasen et al. [14]	
	$\lambda$ (nm)	$\alpha_{\text{OH}}$ (dB/km ppm)	$\lambda$ (nm)	$\alpha_{\text{OH}}$ (dB/km ppm)	$\lambda$ (nm)	$\alpha_{\text{OH}}$ (dB/km ppm)	$\lambda$ (nm) (nm)	$\alpha_{\text{OH}}$ (dB/km ppm)
$\nu_3$	—	—	—	—	2681	10000	2720	10030
$\nu_3 + \nu_1$	—	—	—	—	2203	206.5	2220	195
$\nu_3 + 2\nu_1$	—	—	—	—	—	—	—	—
$2\nu_3$	1370	50.4	—	—	1374	61.9	1380	60.6
$2\nu_3 + \nu_1$	1230	2.6	—	—	—	—	1240	2.63
$2\nu_3 + 2\nu_1$	1125	0.059	—	—	—	—	—	—
$3\nu_3$	950	1.25	945	0.83	938	1.26	940	2
$3\nu_3 + \nu_1$	880	0.115	880	0.075	—	—	—	—
$3\nu_3 + 2\nu_1$	825	0.014	820	0.003	—	—	—	—
$4\nu_3$	725	0.111	720	0.058	—	—	—	—
$4\nu_3 + \nu_1$	685	0.016	680	0.0033	—	—	—	—
$4\nu_3 + 2\nu_1$	—	—	640	0.0008	—	—	—	—
$5\nu_3$	585	0.009	600	0.005	—	—	—	—

<sup>a</sup> The parameters  $\nu_3$  and  $\nu_1$  describe the OH fundamental mode and the  $\text{SiO}_4$  tetrahedron vibration, respectively.

<sup>b</sup> In Ref. [11] Keck et al. used the extinction coefficient of Ref. [13] for the absolute OH content.

<sup>c</sup> Only the measured values from Ref. [12] are listed here.

Gaussian and Lorentzian components [16,22–24]. The components are attributed to three differently bonded hydroxyl groups and one combination mode or to four differently bonded hydroxyl groups, respectively.

### 3. Experimental procedure

#### 3.1. Sample preparation

We prepared bulk samples with 2 mm to 200 mm thickness and optical fibers with lengths between 0.22 m and 1050 m. Thus we were able to adjust the sample length to the strength of the absorption band to be measured. The surfaces of the bulk samples were plane, parallel, and mechanically polished. The multimode step-index optical fibers were drawn from Fluosil<sup>™</sup><sup>1</sup> preforms with 200  $\mu\text{m}$  core and 280  $\mu\text{m}$  outer diameter. The refractive index difference between the undoped core and the fluorine doped cladding varies between  $17 \times 10^{-3}$  and  $22 \times 10^{-3}$ , depending on sample type. Fibers with such high refractive index differences were chosen to minimize the cladding influence on measurement results by reducing the penetration depth of the guided light into the cladding.

Three types of synthetic silica were investigated. Two were produced by flame hydrolysis reaction starting with silicon tetrachloride in an oxyhydrogen torch. The primary  $\text{SiO}_2$  particles form a porous soot body which is vacuum sintered. The obtained synthetic silica has an OH content of about 250 ppm (code name: F310). If a dehydration step is introduced before sintering the OH content is reduced to typically 0.2 ppm (code name: F300). Silica with OH contents of about 700 ppm (code name: F100) was produced by flame hydrolysis and direct melt. F100 and F300 were measured as core materials of optical fibers and as bulk samples. F310 was measured only as bulk material.

#### 3.2. Experimental set-ups

Bulk measurements were performed with a conventional Fourier spectrometer (Perkin Elmer, 2000

FT-IR). The resolution was  $16 \text{ cm}^{-1}$  which is sufficient with respect to the width of the OH bands of about  $200 \text{ cm}^{-1}$  FWHM. Data were averaged over 50 scans.

For fiber measurements two set-ups were used. Equipment A was already described in detail [25,26]. The light is launched from a monochromator into the fiber. The numerical aperture is 0.15 compared to 0.22 of the fiber. The spot size at the fiber front face is about 80% of the core cross section. A monochromator bandwidth of 1 nm was obtained for the entire investigated spectral range between 400 and 1600 nm.

Equipment B includes comparable components arranged in the same sequence as for equipment A. The main differences are the launching conditions and spectral resolution. The numerical aperture of 0.25 is larger than that of the fiber and the spot size of about 40  $\mu\text{m}$  ensures excitation of only meridional fiber modes. Skew rays are suppressed very efficiently. The resolution is 1 nm for wavelengths between 500 and 1100 nm and 4 nm for 1100 to 1700 nm.

All three systems were calibrated with a praseodymium filter having absorption bands between 400 and 1550 nm.

### 4. Results

Bulk spectra of wet (F100) and dry (F300) synthetic silica are shown in Fig. 1. These data are obtained from transmission measurements. Wavelength dependent reflection losses at the surfaces are subtracted. For dry silica with about 0.2 ppm OH even the very strong fundamental mode at about 2.72  $\mu\text{m}$  is not resolved in this scaling. The spectrum of the wet silica is affected by the fundamental mode  $\nu_3$  and the overtones  $2\nu_3$ ,  $3\nu_3$  together with a few combination modes.

Fig. 2 shows the corresponding fiber spectra in the lower wavelength region. For fibers with 1 km length the first overtone at 1383 nm is the dominant feature of the dry silica attenuation spectrum with some further weak OH bands. The basic attenuation is nearly completely governed by Rayleigh scatter-

<sup>1</sup> Fluosil is a registered trademark of Heraeus Quarzglas GmbH.

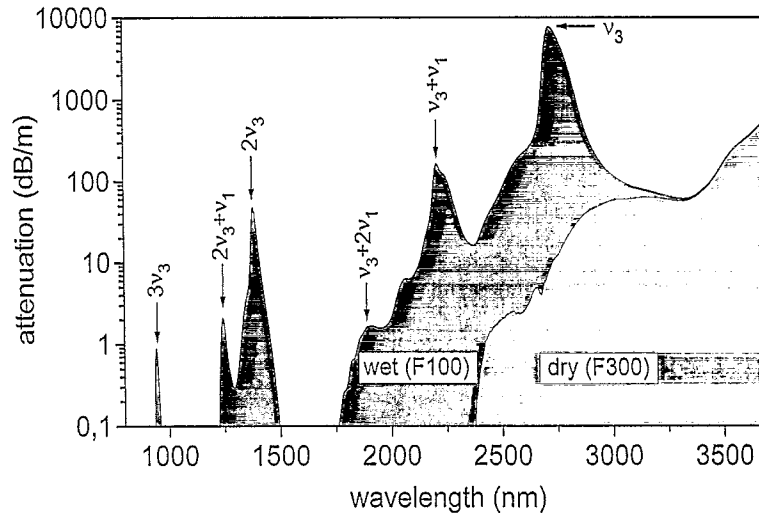


Fig. 1. Bulk attenuation spectra of wet (F100) and dry (F300) synthetic silica.

ing. The wet silica spectrum is a good example for the principle pattern of the OH bands spectral positions and relative intensities. Each of the overtones at 724 nm, 943 nm and 1383 nm is accompanied by two less intense combination modes located at the short wavelength tail of the corresponding overtone absorption band.

As an example for the typical asymmetric shape of an OH absorption band the normalized first over-

tone measured on a wet silica fiber is given in Fig. 3. According to the literature mentioned above, four Gaussians were fitted (see Table 2) to separate the symmetric contributions. Our fits are similar to those of previous work [23,24].

In Fig. 4(a)–(c) measurements on different samples are compared. The first overtone at 1383 nm is plotted together with the combination mode at 1246 nm. Normalization with respect to the intensity of

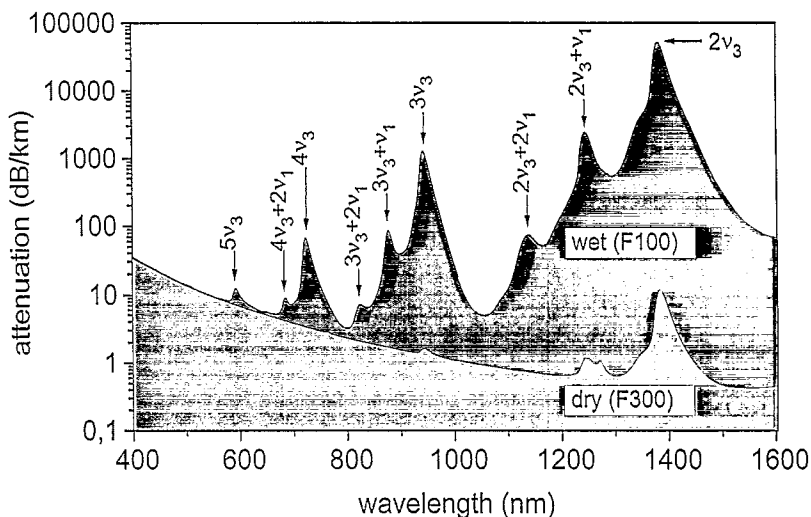


Fig. 2. Attenuation spectra of wet (100) and dry (F300) silica core fibers.

Table 2  
Gaussian fittings of Fig. 3

$i$	$\lambda_i$ (nm)	$\sigma_i$ (nm)	$A_i$
1	1353	20.2	0.058
2	1382	6.7	0.664
3	1393	10.6	0.380
4	1407	29.2	0.132

the first overtone simplifies the analysis of the band shape and the intensity ratio of the two bands.

The comparison of wet fiber and bulk silica data in Fig. 4(a) reveals no differences in band shape or intensity ratio. This similarity indicates that the sample geometry has no influence on OH absorption. To investigate the influence of the silica manufacturing process on the OH absorption one sample produced via direct melting technique is compared to another sample produced by soot technology (Fig. 4(b)). Within the measurement accuracy no differences in band shapes or intensity ratios were observed.

Dry and wet silica are compared in Fig. 4(c). The OH contents differ by more than three orders of magnitude. Nevertheless, good agreement of band shapes and intensity ratios is found. However, a small broadening of the dry material first overtone

peak is observed. The additional peak at 1270 nm is typical for dry silica processed in the preform plasma process. This plasma peak is caused by traces of molecular oxygen in the silica structure [27] and leads to a small increase of the 1246 nm OH band maximum. Our data show no significant influence of OH content on band shape or intensity ratios.

Table 3 provides an overview of all measured data which were calculated as follows. For each OH peak a differential spectrum was calculated by subtracting an exponential base line from the original data. Band intensities and spectral positions of the OH bands were determined from these differential spectra. The experimental error given for the peak intensities reflects the difficulty in determining the attenuation of weak bands located in the tail region of stronger OH bands. All bulk data are normalized to 10000 at 2722 nm (see discussion of literature). Fiber data are fitted to bulk measurements at 1383 nm by normalization to 62.7.

The summary in Table 3 verifies the results shown in Fig. 4(a)–(c) on a broad basis. Band positions were found to be equal within a tolerance of  $\pm 1$  nm. Relative band intensities are independent of sample geometry, OH content, or manufacturing process. Therefore we can summarize the properties of OH

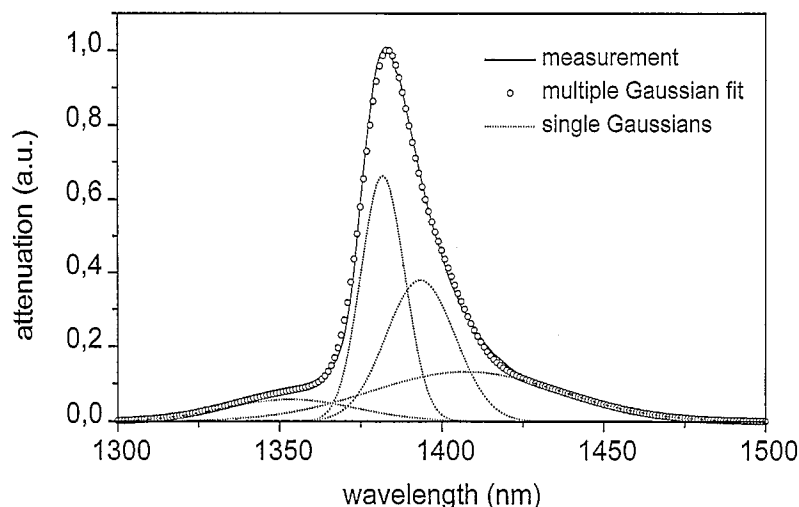


Fig. 3. Normalized first overtone absorption band of wet silica. The measured curve is fitted by four Gaussians with parameters  $\lambda_i$  for center wavelengths,  $\sigma_i$  for peak half widths and  $A_i$  for individual peak amplitudes.

Table 3  
Positions and relative intensities of OH absorption bands in synthetic silica

OH band ident.	$\lambda$ (nm)	Wet silica bulk direct melt $\alpha_{OH}$ (rel.)	Wet silica bulk soot process $\alpha_{OH}$ (rel.)	Wet silica core fiber $\alpha_{OH}$ (rel.)	Dry silica core fiber $\alpha_{OH}$ (rel.)	Result $\alpha_{OH}$ (rel.)	Exp. error
$\nu_3$	$2722 \pm 1$	10000	10000	—	—	10000	—
$\nu_3 + \nu_1$	$2212 \pm 1$	199	202	—	—	201	$\pm 5$
$\nu_3 + 2\nu_1$	$1894 \pm 1$	0.91	0.77	—	—	0.84	$\pm 0.1$
$2\nu_3$	$1383 \pm 1$	62.1	63.3	62.7	62.7	62.7	$\pm 1$
$2\nu_3 + \nu_1$	$1246 \pm 1$	2.62	2.69	2.7	2.9	2.7	$\pm 0.5$
$2\nu_3 + 2\nu_1$	$1139 \pm 1$	0.067	—	0.062	0.08	0.07	$\pm 0.01$
$3\nu_3$	$943 \pm 1$	1.55	1.62	1.5	1.66	1.6	$\pm 0.1$
$3\nu_3 + \nu_1$	$878 \pm 1$	—	—	0.085	0.07	0.08	$\pm 0.02$
$3\nu_3 + 2\nu_1$	$825 \pm 1$	—	—	0.0038	—	0.0038	$\pm 0.0005$
$4\nu_3$	$724 \pm 1$	—	—	0.078	—	0.078	$\pm 0.005$
$4\nu_3 + \nu_1$	$685 \pm 1$	—	—	0.0044	—	0.0044	$\pm 0.0005$
$4\nu_3 + 2\nu_1$	$651 \pm 1$	—	—	0.00028	—	0.00028	$\pm 0.00005$
$5\nu_3$	$593 \pm 1$	—	—	0.0064	—	0.0064	$\pm 0.0005$
$5\nu_3 + \nu_1$	$566 \pm 1$	—	—	0.0003	—	0.0003	$\pm 0.0001$
$6\nu_3$	$506 \pm 1$	—	—	0.0005	—	0.0005	$\pm 0.0002$
$7\nu_3$	$444 \pm 1$	—	—	0.00012	—	0.00012	$\pm 0.00005$

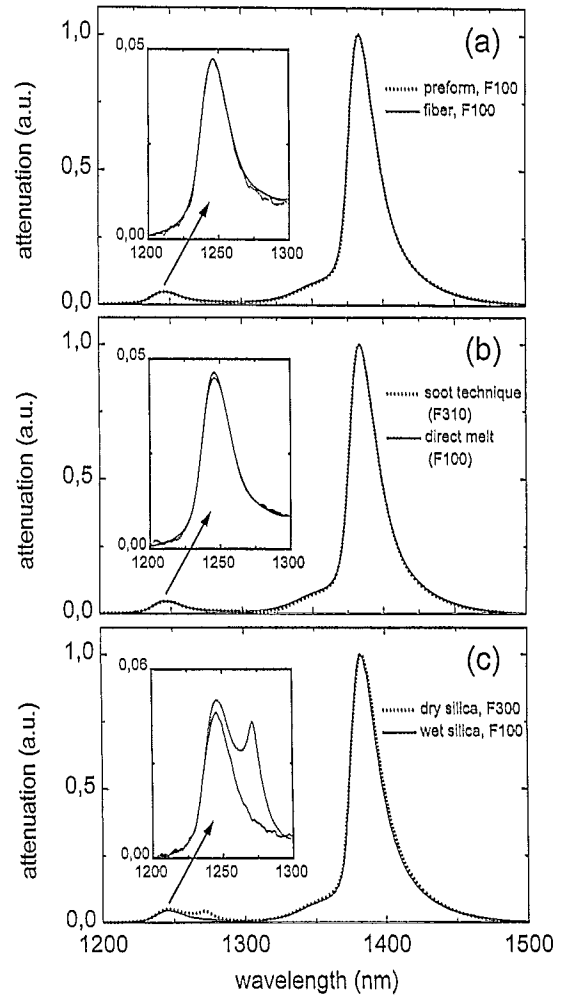


Fig. 4. Comparison of OH absorption bands measured on (a) preform and fiber samples, (b) samples produced by direct melt and soot technique and (c) dry and wet silica.

absorption bands in undoped silica in general as shown in the right part of Table 3.

## 5. Discussion

Our results show that OH absorption bands are quite insensitive to the parameters investigated. Different manufacturing processes and fiber drawing do not affect the OH absorption. The expected influence of the different fictive temperature of bulk and fiber samples on peak position [19,20] was estimated to be less than 1 nm and is therefore not resolved within our measurement accuracy.

The OH content was varied by more than three orders of magnitude but no significant changes of OH band positions, shapes and conversion factors were found. An explanation might be that OH contents of 0.2 ppm and 700 ppm are still small concentrations and the probability to have local areas with modified network structure due to high OH concentrations is small. The OH absorption bands at 506 nm and 444 nm were assigned to the fifth and sixth overtone by a simple approach of an anharmonic oscillator as already done by Elliot and Newns [13].

Overtone frequencies  $\nu_n$  with  $n > 1$  can be calculated by  $\nu_n = n\nu_H[1 - x_A(n + 1)]$  where  $\nu_H$  is the fundamental mode of the harmonic oscillator and  $x_A$  is the anharmonicity constant. With such simple approach it is possible to calculate the wavelength of each overtone with less than 1 nm error. The analysis of our data revealed an anharmonicity constant,  $x$ , of 0.021.

## 6. Conclusion

Relative intensities of the OH absorption bands in synthetic silica were measured between 0.4  $\mu\text{m}$  and 3.6  $\mu\text{m}$  wavelength. To avoid any systematic experimental error two different set-ups were used for fiber measurements as well as a standard FTIR spectrometer for bulk measurements. All samples were chosen from state of the art synthetic silica which is commercially available.

We investigated the influence of the manufacturing process, the OH content and the sample geometry on OH absorption. The spectral position, shape and relative intensity of the OH bands remained unchanged within experimental error. Therefore, we are able to describe the contribution of OH absorption to the overall transmission properties of synthetic silica in general.

We measured the absorption bands of the fifth and sixth OH overtone at 506 nm and 444 nm, respectively. To our knowledge, this is the first time such data are reported.

The results presented provide a lot of opportunities for practical work. They allow to extrapolate between different spectral regions as well as between different sample geometries or materials. Measurements on bulk samples can be used to predict OH

contributions in optical fibers and may allow spacial resolutions not possible in fibers. On the other hand it is possible to use fiber data to determine even extremely low OH concentrations which may have an influence on the performance of bulk optical components in high power laser applications. To estimate the influence of OH bands on transmission windows measurement data on wet silica can be used to determine band shapes very precisely. The model should be transferable to dry silica.

## Acknowledgements

The authors would like to thank H.U. Fisch, M. Flach, S. Ortner and C. Schmitt (Heraeus Quarzglas GmbH) for their work on sample preparation and measurements and H. Strube (Deutsche Telekom AG) for fiber attenuation measurements.

## References

- [1] P.F. Glodis, C.F. Gridley, W.M. Flegal, A.A. Klein, D.P. Jablonowski, D. Kalish, A. Sorby, H. Damsgaard, G. Knudsen, H. Schaper, N. Treber, H. Fabian and P.C. Schulz, in: Proc. 43rd Int. Wire and Cable Symp., Atlanta Proc. (IWCS, Eaton Town, NJ, 1994) p. 105.
- [2] A.J. Stephenson and K.H. Jack, Trans. Br. Ceram. Soc. 59 (1960) 397.
- [3] G. Hetherington and K.H. Jack, Phys. Chem. Glasses 3 (1962) 129.
- [4] K.M. Davis, A. Agarwal, M. Tomozawa and K. Hirao, these Proceedings, p. 27.
- [5] H. Eberdorff-Heidepriem and D. Ehrhart, Glastechn. Ber. Glass Sci. Technol. 68 (1995) 139.
- [6] J.E. Shelby, J. Vitko Jr., and R.E. Benner, J. Am. Ceram. Soc. 65 (1982) C59.
- [7] Y. Morimoto, T. Igarashi, H. Sugahara and S. Nasu, J. Non-Cryst. Solids 139 (1992) 35.
- [8] G.H.A.M. van der Steen and E. Papanikolaou, Philips Res. Rep. 30 (1975) 192.
- [9] J.P. Williams, Y.-S. Su, W.R. Strzegowski, B.L. Butler, H.L. Hoover and V.O. Altemose, Am. Ceram. Soc. Bull. 55 (1976) 524.
- [10] D.B. Keck, R.D. Maurer and P.C. Schultz, Appl. Phys. Lett. 22 (1973) 307.
- [11] D.B. Keck and A.R. Tynes, Appl. Opt. 11 (1972) 1502.
- [12] P. Kaiser, A.R. Tynes, H.W. Astle, A.D. Pearson, W.G. French, R.E. Jaeger and A.H. Cherin, J. Opt. Soc. Am. 63 (1973) 1141.
- [13] C.R. Elliott and G.R. Newns, Appl. Spectrosc. 25 (1971) 378.

- [14] R. Clasen, *Glastech. Ber.* 63 (1990) 291.
- [15] J. Stone and G.E. Walrafen, *J. Chem. Phys.* 76 (1982) 1712.
- [16] M. Bredol, D. Leers, L. Bosselaar and M. Hutjens, *J. Lightwave Technol.* 8 (1990) 1536.
- [17] N. Uchida and N. Uesugi, *J. Lightwave Technol.* 4 (1986) 1132.
- [18] R. Brückner, *J. Non-Cryst. Solids* 5 (1970) 123.
- [19] A.E. Geissberger and F.L. Galeener, *Phys. Rev. B* 28 (1983) 3266.
- [20] A. Agarwal, K.M. Davis and M. Tomozawa, *J. Non-Cryst. Solids* 185 (1995) 191.
- [21] K.M. Davis and M. Tomozawa, *J. Non-Cryst. Solids* 185 (1995) 203.
- [22] G.E. Walrafen and S.R. Samanta, *J. Chem. Phys.* 69 (1978) 493.
- [23] S.S. Walker, *J. Lightwave Technol.* 4 (1986) 1125.
- [24] Y. Yokomachi, R. Tohmon, K. Nagasawa and Y. Ohki, *J. Non-Cryst. Solids* 95&96 (1987) 663.
- [25] W. Heitmann, *J. Opt. Commun.* 8 (1987) 2.
- [26] W. Heitmann, *J. Opt. Commun.* 11 (1990) 122.
- [27] W. Carvalho, P. Dumas, J. Corset and V. Neuman, *J. Raman Spectrosc.* 16 (1985) 330.